



Title	Alternative AEFIE-EFIE Method for Broadband CEM Modeling
Author(s)	Liu, J; Jiang, L
Citation	The I E E E International Symposium on Electromagnetic Compatibility (EMC), Pittsburgh, USA, 6-10 August 2012. In International Symposium on Electromagnetic Compatibility Proceedings, 2012, p. 515-520
Issued Date	2012
URL	http://hdl.handle.net/10722/186726
Rights	International Symposium on Electromagnetic Compatibility Proceedings. Copyright © I E E E.

Alternative AEFIE-EFIE Method for Broadband CEM Modeling

Jia Liu^{1,2} and Li Jun Jiang¹

1. Department of Electrical and Electronic Engineering, University of Hong Kong, Hong Kong, 999077.

Email: jianglj@hku.hk

2. Department of electronic and information engineering, Beihang university, Bei Jing, 100191, China.

Email: liujia1985219@gmail.com

Abstract—It is well known that the electric field integral equation (EFIE) has the low frequency breakdown problem while the Augmented electric field integral equation (AEFIE) method has the high frequency breakdown issue. To obtain a unified method that works for both low and high frequencies without manual switching of methods, a novel and simple method is proposed in this paper. It uses AEFIE and EFIE to compensate each other iteratively in all frequency regimes to guarantee the accuracy of the solution. As a result, it effectively extends AEFIE to the high frequency regime and extends EFIE to the low frequency regime. Numerical results demonstrated that this alternative AEFIE-EFIE method is able to extend integral equations to broad band applications.

I. INTRODUCTION

In computational electromagnetic (CEM), integral equation methods are frequently employed for various applications including transmission line systems, scattering objects, and microwave components. However, the low frequency breakdown of the electric field integral equation (EFIE) based on the method of moments (MOM)^[1] seriously limited its applications, especially those related to EMC and EMI characterizations happening in a very wide frequency range. Several methods have been used to solve this issue. Among them, the loop-tree decomposition^[2-3] seems to be the most effective remedy that separates the electrostatic and magnetic physics to build a well-conditioned numerical system. However, searching loops in complex geometries is very time consuming. Other efforts have been made to achieve stable formulas without the loop-tree searching. The current and charge integral equation (CCIE)^[4] and the separated potential integral equation (SPIE)^[5] are successful examples that separate current and charge to enforce both KCL and KVL laws in the circuit physics.

Augmented electric field integral equation (AEFIE)^[6] also takes current and charge as unknowns and uses current continuity equation as

the connection between them. Many numerical results prove AEFIE could perform very well in the low frequency regime using the conventional RWG basis^[7]. Hence, it is suitable for complicated EMC and EMI analysis. However, with increasing working frequencies and high order noise harmonics, the convergence of AEFIE degrades. This seriously affects its calculation of large scale problems at high frequencies.

To obtain a unified broadband method, this paper proposes a novel but rather simple alternative AEFIE-EFIE method. It uses EFIE to complement AEFIE system to achieve better convergence performance in the higher frequency range. The complementary terms for the current and the charge in AEFIE are calculated based on the linearity of the electromagnetic system. Numerical results demonstrate that this method has very good convergence over broad frequency range. It can achieve a satisfactory compromise between AEFIE and EFIE. This method effectively extends AEFIE for high frequency problems and extends EFIE for low frequency problems.

II. EFIE AND AEFIE

The conventional EFIE can be written as

$$(ik_0\eta_0\bar{V} + \frac{\eta_0}{ik_0}\bar{S}) \cdot J = b \quad (1)$$

where k_0 and η_0 are the wave number and intrinsic impedance respectively. Vector J represents the current coefficient, vector b represents the excitation, \bar{V} is the vector potential matrix, and \bar{S} is the scalar potential matrix.

The basic AEFIE is of the form

$$\begin{bmatrix} \bar{\bar{V}} & \bar{\bar{D}} \cdot \bar{\bar{P}} \\ \bar{\bar{D}} & k_0^2 \bar{\bar{I}} \end{bmatrix} \cdot \begin{bmatrix} ik_0 \cdot \bar{\bar{J}} \\ c_0 \cdot \bar{\bar{\rho}} \end{bmatrix} = \begin{bmatrix} \eta_0^{-1} \cdot \bar{b} \\ 0 \end{bmatrix} \quad (2)$$

where $\bar{\bar{I}}$ is an identity matrix, $\bar{\rho}$ is the charge vector, $\bar{\bar{D}}$ is the incidence matrix. Equation (2) clearly highlights AEFIE method's circuit physical nature. There are also other AEFIE formulas corresponding to various applications.

In the low frequency range, the coupling between the electric field and the magnetic field is very weak. This is due to the Helmholtz decomposition, which is the motivation of the AEFIE formulation. However, when the frequency is increasing, the coupling between electric field and magnetic field becomes stronger. Wave physics will replace the circuit physics. The Helmholtz decomposition becomes improper to characterize the high frequency phenomenon.

Meanwhile, EFIE has exactly the opposite problem that is known as the low frequency breakdown. It was due to over emphasizing of the potential contribution due to the frequency scaling in EFIE.

Fig. 1 illustrates the condition number comparison between AEFIE and EFIE in a wide frequency range for a one meter PEC sphere. Both of them use GMRES as the iterative method. Apparently EFIE is better conditioned than AEFIE in the higher frequency range while AEFIE is more stable in the low frequency regime.

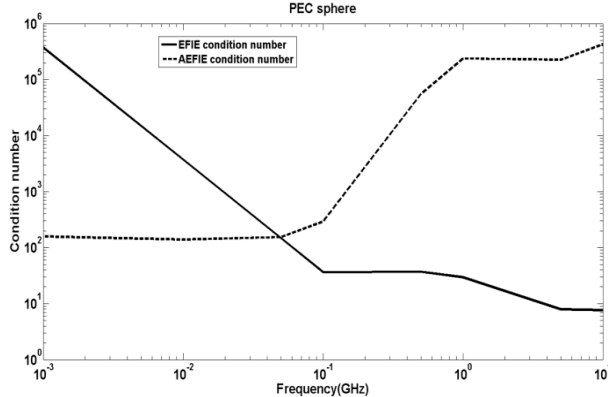


Figure.1 Condition number comparison between AEFIE and EFIE for a unit PEC sphere.

III. ALTERNATIVE AEFIE-EFIE METHOD

From the analysis in Part II, it is natural to consider combining the advantages of AEFIE and

EFIE to achieve a true broadband analysis. The implementation of this idea is based on the linearity of the electromagnetic system.

For simplicity, AEFIE and EFIE operators are replaced by matrix symbols:

$$[\text{AEFIE}] \begin{bmatrix} ik_0 \bar{J} \\ c_0 \bar{\rho} \end{bmatrix} = \begin{bmatrix} \eta^{-1} \cdot \bar{b} \\ 0 \end{bmatrix} \quad (3a)$$

$$[\text{EFIE}] \cdot \bar{J} = \bar{b} \quad (3b)$$

Suppose AEFIE equation (3a) is solved first without considering its frequency instability issue at all. The resultant current and charge are represented by \bar{J}_1 and $\bar{\rho}_1$ respectively. In the low frequency regime, \bar{J}_1 and $\bar{\rho}_1$ are very accurate due to the good condition number of AEFIE. But in the higher frequency regime, their numerical accuracies are expected to be bad. If \bar{J} and $\bar{\rho}$ are the real solutions of equation (3a), the residual error vector can be calculated by the following equation:

$$\begin{aligned} [\text{AEFIE}] \begin{bmatrix} ik_0 (\bar{J} - \bar{J}_1) \\ c_0 (\bar{\rho} - \bar{\rho}_1) \end{bmatrix} &= \begin{bmatrix} \eta^{-1} \cdot \bar{b} \\ 0 \end{bmatrix} - [\text{AEFIE}] \begin{bmatrix} ik_0 \bar{J}_1 \\ c_0 \bar{\rho}_1 \end{bmatrix} \\ &= \Delta \text{AEFIE} \end{aligned} \quad (4)$$

This residual error cannot be accurately calculated at high frequencies when AEFIE's numerical performance is not good. In this situation, EFIE equation (3b) can be used. Because EFIE only takes the current as unknowns, the initial solution \bar{J}_1 from AEFIE will be used in (3b). By the comparison with the true solution in EFIE, we have

$$\begin{aligned} [\text{EFIE}] \cdot \bar{J} - [\text{EFIE}] \cdot \bar{J}_1 &= \\ \bar{b} - [\text{EFIE}] \cdot \bar{J}_1 &= \Delta \text{EFIE} \end{aligned} \quad (5)$$

ΔEFIE is the field residual error due to the inaccuracy of \bar{J}_1 . It is directly related to the current residual error as in the following equation:

$$[\text{EFIE}] \cdot \Delta \bar{J} = \Delta \text{EFIE} \quad (6)$$

Hence, the current deviation $\Delta\bar{J}$ between the real solution and \bar{J}_1 can be achieved through equation (6). $\Delta\bar{J}$ is further used to correct \bar{J}_1 to obtain a better solution:

$$\bar{J}_2 = \bar{J}_1 + \Delta\bar{J} \quad (7)$$

\bar{J}_2 is the corrected solution to (3a) complemented by (3b). If the deviation $\Delta\bar{J}$ is not small enough to be within certain tolerance, the whole AEFIE-EFIE process will be iterated again.

As for the charge term, because EFIE cannot complement it directly, the current continuity equation is employed:

$$\bar{\bar{D}} \cdot \Delta\bar{J} = ik_0 c_0 \Delta\bar{\rho} \quad (8)$$

Because the incidence matrix $\bar{\bar{D}}$ is diagonal dominant, solving equation (8) needs $O(N)$ computation sources with controllable error. As a result, $\Delta\bar{\rho}$ is used as the correcting term for the first charge solution $\bar{\rho}_1$:

$$\bar{\rho}_2 = \bar{\rho}_1 + \Delta\bar{\rho} \quad (9)$$

The complementing process introduced above is expected to give better results than \bar{J}_1 and $\bar{\rho}_1$ from AEFIE for high frequencies but worse results for low frequencies. If the resulting \bar{J}_2 and $\bar{\rho}_2$ is not good enough, the process will be further repeated until the error is within certain tolerance.

From the first glance of this proposed process, it is easy to believe that it will increase the computation cost because it involves both AEFIE and EFIE calculations. However, its actual implementation showed that its computation cost is aggravated with acceptable amount. Under the same residual requirement, its iteration number could be between EFIE and AEFIE, and closer to the better one.

The biggest advantage of this proposed scheme is its uniform process for both low and high frequencies without a check for the electrical size of the object. The method could validate the better one between EFIE and AEFIE automatically over wider

frequency range so that more resources can be put on the optimal one to achieve the convergence. It uses regular RWG basis through the spectrum. And it is extremely easy to be implemented based on existing integral equation methods. Its resultant performance is definitely not the optimal but is close to the optimal through this unified process. Numerical results in next part highlight its performance especially in higher frequency range in which AEFIE could hardly give satisfied results. Wide band simulations could be implemented without manually switching the method between AEFIE and EFIE, which is difficult to determine in the transition region.

IV. NUMERICAL RESULTS

In this part, some numerical examples are tested to demonstrate the effectiveness of the proposed alternative AEFIE-EFIE method. Fig. 2 and 3. give the iteration numbers of AEFIE, EFIE and the alternative AEFIE-EFIE method for a PEC sphere (with 1 meter radius) and a PEC cube (with 1 meter edge). The relative error residual is set to 1×10^{-12} . It is seen that EFIE and AEFIE only maintain a reasonable iteration number for certain frequency range. But the alternative AEFIE-EFIE can keep a relatively flat iteration cost for all frequency range. The peak around 500MHz is due to the cavity resonance. Overall the iteration number of the alternative AEFIE-EFIE method is much closer to the optimal one – at low frequencies it is closer to AEFIE while at high frequencies it is closer to EFIE. The differences among three methods are more obvious in higher frequency regime. In Fig 2, the AEFIE method could not reach the convergence, while the more involvement of EFIE could help the alternative process reach the convergence. The similar situation also exists in PEC cube case.

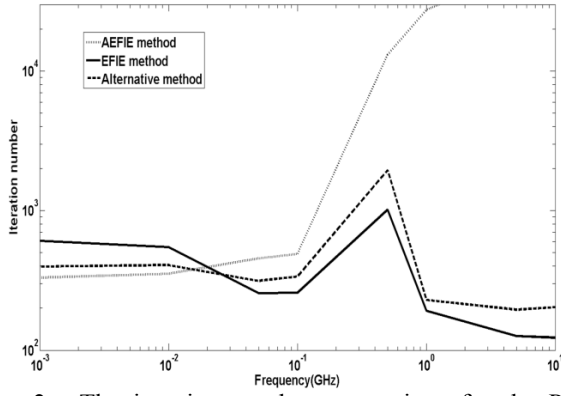


Figure 2. The iteration number comparison for the PEC sphere.

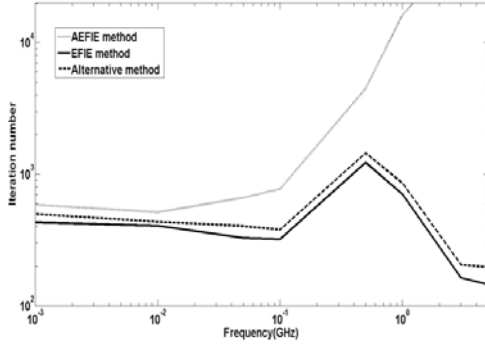


Figure 3. The iteration number comparison for a PEC cube.

In the Fig. 4 and 5, the iteration number is set to 100 to compare the residual error reduction speed of EFIE, AEFIE and the alternative AEFIE-EFIE method over a broad frequency range. With the increment of frequency, AEFIE is gradually outperformed by EFIE in the residual error reduction under limited iteration. The residual error from the alternative AEFIE-EFIE method is in between of EFIE and AEFIE.

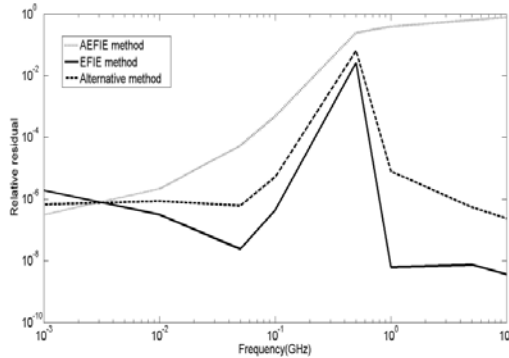


Figure 4. The residual error comparison for the PEC sphere.

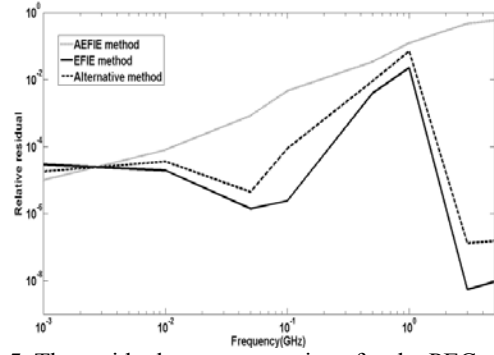


Figure 5. The residual error comparison for the PEC cube

To see the differences of these three methods, the current distributions on a PEC sphere was calculated, as shown in Fig. 6. The sphere's radius is 1×10^{-5} wavelength. Due to the low frequency breakdown in EFIE, the current distribution difference between AEFIE and EFIE is obvious, and the alternative method agrees with that of AEFIE very well. Fig. 7 shows the comparison for a sphere with the radius of 10 wavelengths. Since AEFIE could not converge for such a high frequency problem, EFIE gives a more reliable result. The last plot in Fig. 7 shows that the alternative method proposed in this paper agrees very well with the result of EFIE at higher frequency.

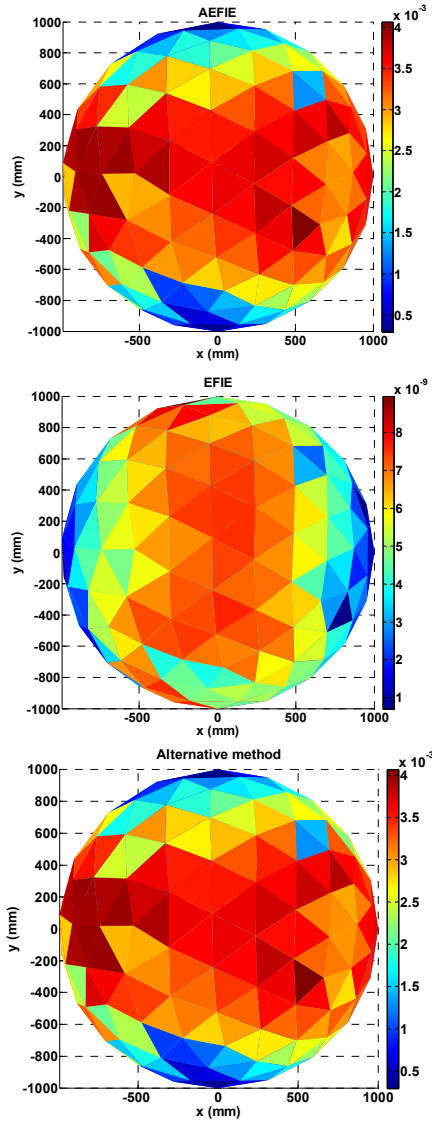


Figure 6. The current distribution comparison when the sphere radius is 1×10^{-5} wavelength.

Another example for validation is the thin strip antenna with 2m length and 0.02m width. The delta gap source is added in the middle of the antenna. Due to the small number of the patch discretization, bi-conjugate gradient iteration method is taken with the relative residual 1×10^{-10} . Fig. 8 and Fig. 9 demonstrate the iteration numbers and computation time of the three methods. The alternative method achieves acceptable compromise performance as in the case of PEC sphere and cube. Fig. 10 and Fig. 11 demonstrate the current distribution of the antenna in low and high frequencies. It is seen that

the result from the alternative method is close to the optimal method in the different frequency bands.

More results will be shown at the conference.

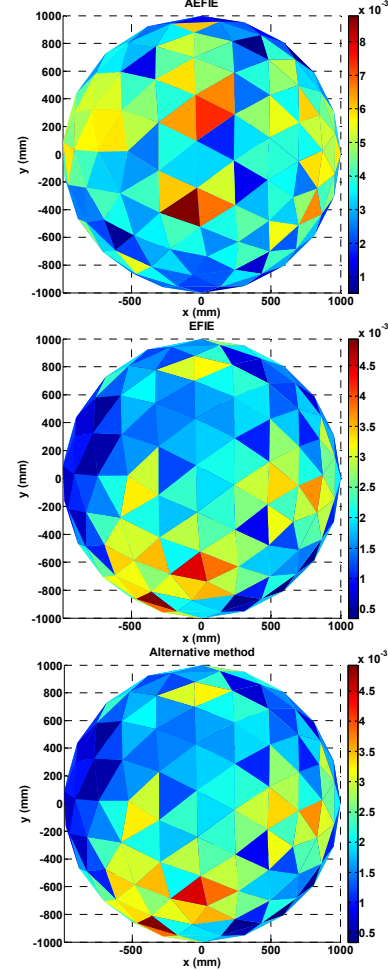


Figure 7. The current distribution comparison when the sphere radius is 10 wavelengths.

V. CONCLUSION

To overcome the high frequency breakdown of AEFIE and low frequency breakdown of EFIE, a novel unified integral equation approach, alternative AEFIE-EFIE method, is proposed to deliver the broadband accuracy and stability without using loop-tree decomposition and manual switching for different frequencies. It employs AEFIE and EFIE to compensate each other in both high and low frequency regimes. As a result, through a unified and simple iteration process, the integral equation method can conveniently cover both high and low frequency applications with very

good accuracy in a computation cost closer to optimal in each frequency regime.

VI. ACKNOWLEDGEMENT

We thank Professor W.C. Chew for his constructive helps. Also we are grateful to the supports from HKU Seed Fund 201001159006, HKU Small Project Fund 201007176196, GRF713011, and the University Grant Council (AoE/P-04/08).

REFERENCES

- [1] R.F.Harrington, *Field Computation by Moment Methods*, IEEE Press, New York, 1993.
- [2] D.R.Wilton, J.S.Lim, and S.M.Rao, "A novel technique to calculate the electromagnetic scattering by surfaces of arbitrary shape," *URSI Radio Science Meeting*, Ann Arbor, MI, June 1993, p.322.
- [3] G.Vecchi, "Loop-star decomposition of basis functions in the discretization of the EFIE," *IEEE Trans Antennas Propag*, vol. 47, pp 339-346, 1999.
- [4] M.Taskinen and P.Yia-Oijala, "Current and charge integral equation formulation," *IEEE Trans Antennas Propag* 54(2006), 58-67.
- [5] D.Gope, A.R.Ruehli, and V.Jandhyala, "Solving low-frequency EM-CKT problems using the PEEC method," *IEEE Trans Adv Packag* vol. 30, pp 313-320, 2007.
- [6] Z.G.o Qian and W.C. Chew, "Fast full-wave surface integral equation solver for multiscale structure modeling," *IEEE Trans Antennas Propag*, vol. 57, pp3594-3601, 2009.
- [7] S.M.Rao, D.R.Wilton, and A.W.Glisson, "Electromagnetic scattering by surface of arbitrary shape," *IEEE Trans Antennas Propag*, vol. 30, pp 409-418, 1982.

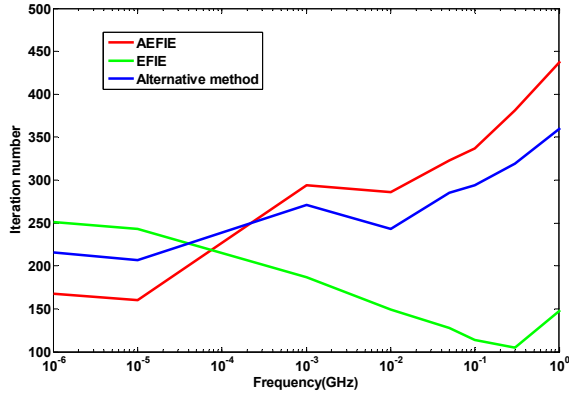


Figure 8. Iteration number comparison for the strip antenna simulation

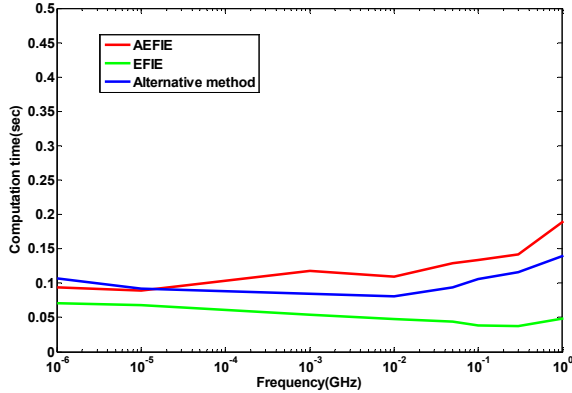


Figure 9. Computation time comparison of the strip antenna model.

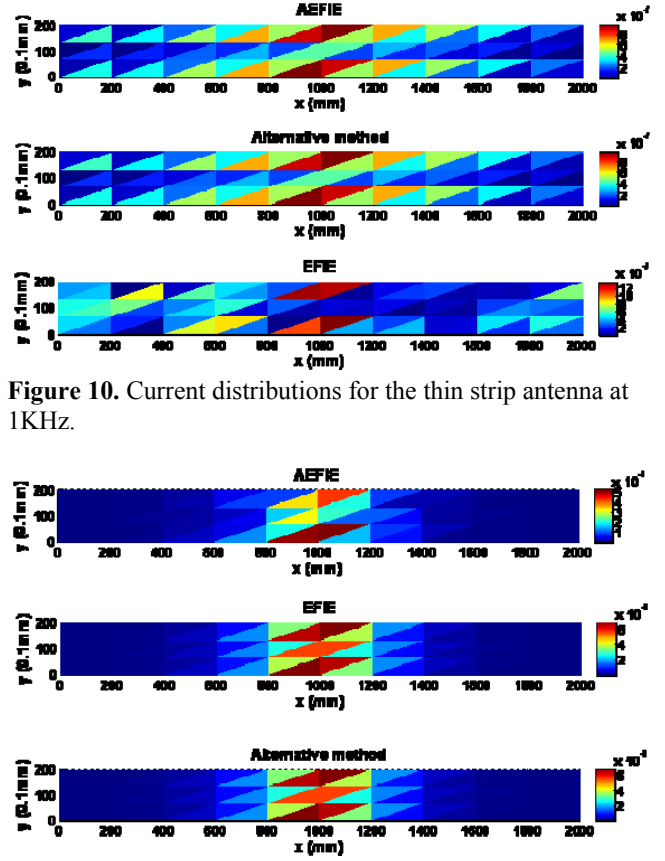


Figure 10. Current distributions for the thin strip antenna at 1KHz.

Figure 11. Current distributions for the thin strip antenna at 1GHz.